[CANCER RESEARCH 62, 3530–3537, June 15, 2002]

Insulin-like Growth Factor Binding Protein-3 Inhibits the Growth of Non-Small Cell Lung Cancer

Ho-Young Lee,[1] Kyung-Hee Chun, Bingrong Liu, Sandra A. Wiehle, Richard J. Cristiano, Waun Ki Hong, Pinchas Cohen, and Jonathan M. Kurie

Departments of Thoracic/Head and Neck Medical Oncology [H-Y. L., K-H. C., W. K. H., J. M. K.] and Genitourinary Medical Oncology [S. A. W., R. J. C.], The University of Texas M. D. Anderson Cancer Center, Houston, Texas 77030, and Department of Pediatrics, Mattell Children's Hospital, University of California, Los Angeles, California 90095-1752 [B. L., P. C.]

ABSTRACT

Insulin-like growth factors (IGFs) have mitogenic and antiapoptotic properties and have been implicated in the development of lung cancer. The effects of IGFs are modulated by insulin-like growth factor binding proteins (IGFBPs). This study explored the effects of IGFBP-3 on non-small cell lung cancer (NSCLC) cells after infection with an adenovirus constitutively expressing IGFBP-3 under the control of the cytomegalovirus promoter (Ad5CMV-BP3). We found that IGFs, especially IGF-I, stimulated the growth of NSCLC cells, and Ad5CMV-BP3 suppressed this IGF-I-induced NSCLC cell growth. We also found that the clonogenicity of H1299 cells in soft agar was markedly reduced by Ad5CMV-BP3. Furthermore, direct injection of Ad5CMV-BP3 into H1299 NSCLC xenografts s.c. established in athymic nude mice induced massive destruction of the tumors. Ad5CMV-BP3 did not induce detectable cytotoxicity on normal human bronchial epithelial cells, suggesting therapeutic efficacy of this virus. Ad5CMV-BP3 infection was accompanied by apoptotic cell death *in vitro* as detected by flow cytometry, DNA fragmentation analysis, and Western blot analysis on the expression of Bcl-2 and on the cleavage of poly(ADP-ribose) polymerase, a substrate of caspase 3. Immunofluorescence confocal microscopy was also used to show the apoptotic effect of Ad5CMV-BP3 in H1299 tumors established in nude mice. These findings indicated that IGFBP-3 was a potent inducer of apoptosis in NSCLC cells *in vitro* and *in vivo*. To delineate the underlying mechanism, we examined the effect of IGFBP-3 on Akt/protein kinase B and glycogen synthase kinase-3β, downstream mediators of the phosphatidylinositol 3-kinase pathway, and on mitogen-activated protein kinase (MAPK), all three of which are activated by IGF-mediated signaling pathways and have important roles in cell survival. IGFBP-3 overexpression inhibited the phosphorylation of Akt and glycogen synthase kinase-3β and the activity of MAPK. Furthermore, IGF-I rescued the NSCLC cells from serum depletion-induced apoptosis, and this rescue was blocked in Ad5CMV-BP-3-infected H1299 NSCLC cells. Transient transfection with activated Akt or constitutively active MAPK kinase-1, an upstream activator of MAPK, partially blocked IGFBP-3-induced apoptosis of NSCLC cells. These findings suggested that the growth-regulatory effect of IGFBP-3 on NSCLC cells was attributable in part to the inhibition of the IGF-induced survival pathway. These data demonstrate the importance of IGFBP-3 in the regulation of NSCLC cell proliferation, clonogenicity, and tumor growth, suggesting that IGFBP-3 is a target for the treatment of lung cancer and that Ad5CMV-BP3 is a potential therapeutic agent.

INTRODUCTION

NSCLC[2] accounts for about 75–80% of lung cancer cases and carries a 5-year survival rate of about 10–15% for all stages (1). Surgical resection is the treatment of choice for patients with stage I or II cancer, whereas patients with later stages of disease are treated with combinations of surgery, chemotherapy, and radiation therapy, all of which have significant side effects. Despite these treatments, the survival rate of patients with NSCLC remains low (2), and new treatment strategies are urgently needed.

Several lines of evidence implicate IGFs and their receptor, IGF-1R, in many human malignancies, including carcinomas of the lung (3). Two distinct signal transduction pathways have been identified for IGF-1R. One pathway activates Ras, Raf, and MAPK, the main mitogen-conducting pathway, and the other pathway involves PI3K, which is responsible for antiapoptotic signal transduction (4). Therefore, we hypothesized that blocking the interaction of IGFs with IGF-1R or interrupting the signal transduction pathway of IGF-1R can abolish the mitogenic activity of IGFs on lung cancer.

IGFBP-3, one of six members of the IGFBP family, regulates bioactivity of IGFs by sequestering IGFs away from its receptor in the extracellular milieu, thereby inhibiting the mitogenic and antiapoptotic action of IGFs (5–7). A negative correlation between serum IGFBP-3 levels and lung cancer risk (6) suggests a protective role of IGFBP-3 against the effects of systemic IGFs. IGFBP-3 also has IGF-independent antiproliferative and proapoptotic effects, as shown by the finding that IGFBP-3 overexpression inhibits the growth of IGF-1R null fibroblasts (7). These effects of IGFBP-3 are probably mediated by other cell surface receptors, such as the TGF-β receptor (8). However, the intracellular mechanisms by which IGFBP-3 mediates its IGF-independent antiproliferative and proapoptotic effects remain largely unknown. It has been demonstrated that IGFBP-3 is translocated to the nucleus, where it could exert a direct influence on gene expression (9, 10); thus, nuclear IGFBP-3 may mediate its IGF-independent cellular effects via direct or indirect interaction with growth-inhibitory genes, apoptotic genes, or both.

IGFBP-3 gene expression has been shown to be induced by growth-inhibitory (and apoptosis-inducing) agents such as TGF-β1 (11), tumor necrosis factor-α (12), retinoic acid (13), anti-estrogen ICI 182780 (14), vitamin D and its analogues EB1089 and CB1093 (15), and the transcription factor p53 (16). Thus, these agents may mediate their cellular effects through IGFBP-3.

IGFBP-3 also can potentiate IGF bioactivity in several different cell types (17, 18). Although the mechanism for the enhancement of the activity of IGF is largely unknown, it is thought to occur after the association of IGFBP-3 with the cell membrane, thereby facilitating the binding of IGFs to its receptor (19). Alternatively, surface-associated IGFBP-3 may be targeted for proteolysis into fragments that have reduced IGF affinity (20). Whether IGFBP-3 assumes an inhibitory role or an enhancing role may depend on the cell type and the compound that induces its expression.

Received 10/3/01; accepted 4/12/02.

The costs of publication of this article were defrayed in part by the payment of page charges. This article must therefore be hereby marked *advertisement* in accordance with 18 U.S.C. Section 1734 solely to indicate this fact.

[1] To whom requests for reprints should be addressed, at Department of Thoracic/Head and Neck Medical Oncology, Box 432, The University of Texas M. D. Anderson Cancer Center, 1515 Holcombe Boulevard, Houston, TX 77030. Phone: (713) 792-6363; Fax: (713) 796-8655; E-mail: hlee@mdanderson.org.

[2] The abbreviations used are: NSCLC, non-small cell lung cancer; IGF, insulin-like growth factor; IGF-1R, IGF-1 receptor; IGFBP, IGF binding protein; MAPK, mitogen-activated protein kinase; MAPKK, MAPK kinase; PI3K, phosphatidylinositol 3-kinase; TGF, transforming growth factor; CMV, cytomegalovirus; PKB, protein kinase B; NHBE, normal human bronchial epithelial; GSK, glycogen synthase kinase; ERK, extracellular signal-regulated kinase; MTT, 3-(4,5-dimethylthiazol-2-yl)-2,5-diphenyltetrazolium bromide; TUNEL, terminal deoxynucleotidyl transferase-mediated dUTP-biotin nick-end labeling; MBP, myelin basic protein; PARP, poly(ADP-ribose) polymerase; FACS, fluorescence-activated cell sorter.

We investigated the effects of overexpression of IGFBP-3 on NSCLC cells using an adenoviral vector as a gene-delivery system. We demonstrated that infection with an adenovirus expressing IGFBP-3 under the control of the CMV promoter (Ad5CMV-BP3) inhibited the growth of NSCLC cells *in vitro* and *in vivo* by inducing apoptosis. We also found that IGFBP-3 is a potent inhibitor of the PI3K/Akt/PKB and MAPK signaling pathways, which are important mediators of cell survival. These findings suggest that IGFBP-3 is a potential target for lung cancer treatment.

MATERIALS AND METHODS

Animals, Cells, and Materials. Female nude mice, 4 weeks of age, were purchased from Harlan-Sprague Dawley (Indianapolis, IN). NHBE cells were grown from the bronchial epithelium as described previously (21). NSCLC cell lines (H1299, H661, H596, A549, H460, H358, H322, H226Br, H226B, Calu6, Calu1, ChagoK, and SK-MES-1) were routinely maintained in RPMI 1640 supplemented with 10% FCS (Life Technologies, Inc., Gaithersburg, MD) in a humidified environment with 5% CO_2. 293 cells were maintained in DMEM containing 10% FCS (Life Technologies, Inc.). Total IGF-I and IGF-II were purchased from R&D Systems, Inc. (Minneapolis, MN). Fluorolink Cy3-labeled secondary antibody was purchased from Amersham Corp. (Arlington Heights, IL), and rabbit polyclonal antibodies against human anti-pAKT (Ser-473), Akt, and pGSK-3β (Ser-9) were purchased from New England Biolabs (Beverly, MA). Rabbit polyclonal anti-GSK-3β antibody (BD Transduction Laboratories, Lexington, KY), rabbit polyclonal anti-Bax and anti-caspase-3 antibodies (PharMingen, San Diego, CA), rabbit polyclonal anti-Bcl-2 and rabbit polyclonal anti-PARP antibody (VIC 5; Roche Molecular Biochemicals, Indianapolis, IN), rabbit polyclonal anti-IGFBP-3 (Santa Cruz Biotechnology, Inc., Santa Cruz, CA), goat antibodies against ERK-1, ERK-2, and β-Actin (Santa Cruz Biotechnology, Inc.), and goat polyclonal antihuman IGFBP-3 antibody (Diagnostic Systems Laboratories, Webster, TX) were used for Western blot analysis or immunofluorescence confocal microscopy. The expression construct pCMV6.MyrAktHA containing a myristoylation sequence fused in-frame to the c-Akt coding sequence (MyrAkt) was a gift from Dr. Gordon Mills (The University of Texas M. D. Anderson Cancer Center). The expression vector pCMV.MCL⊕HA-MAPKK (MEK1/R4F) was a gift from Dr. Melanie Cobb (The University of Texas at Southwestern Medical Center, Dallas, TX).

Generation of Ad5CMV-BP3. A full-length human IGFBP-3 cDNA was inserted into the 5′ end of the bovine growth hormone polyadenylation signal at *Eco*RV of the pAd-shuttle vector. The IGFBP-3-containing shuttle vector was digested with *Bst*B1/*Cla*I, inserted into the pAd-speed vector containing adenoviral DNA, and transfected into 293 cells. 293 cells were maintained in DMEM containing 10% FCS until the onset of the cytopathic effect. The presence of IGFBP-3 was confirmed by dideoxy-DNA sequencing and Western blot analysis. Viral titers were determined by plaque assays and spectrophotometric analysis. The pAd-shuttle vector and pAd-speed vector were kindly provided by Dr. Jack A. Roth (The University of Texas M. D. Anderson Cancer Center).

Western and Western Ligand Blot Analyses. Conditioned media were collected from H1299 cells after adenoviral infection. Western blot and Western ligand blot analyses were performed using 30 μg of whole cell lysate or 30 μl of conditioned media as described previously (22).

Measurements of Cell Growth. To measure the effects of IGF-I and IGF-II on proliferation of NSCLC cells, 2×10^3 NSCLC cell lines were incubated in serum-free medium containing 0.01–500 ng/ml IGF-I or IGF-II for 3 days. To measure the effects of Ad5CMV-BP-3 on proliferation of NHBE and NSCLC cell lines, these cells were seeded at 1×10^3 to 2×10^3 cells/well in 96-well plates. After 1 day, cells were untreated or infected with 1×10^3, 5×10^3, or 1×10^4 particles/cell of Ad5CMV-BP3 or Ad5CMV (parental virus) as a viral control. Infection was allowed to occur for 2 h in the absence of serum, and infected cells were grown in medium containing 100 or 250 ng/ml IGF-I. After 3 days of incubation, the growth of infected cells was measured by the MTT assay as previously described (22).

Growth in Soft Agar. The ability of NSCLC cells infected with Ad5CMV-BP3 to grow in anchorage independence was assessed in soft agar. Briefly, 1×10^3 H1299 cells were transduced with 1×10^3 or 1×10^4 particles/cell of Ad5CMV or Ad5CMV-BP3 for 1 day. They were then suspended in 1 ml of RPMI 1640 containing 10% FCS and 0.2% agarose and were plated in 12-mm tissue culture plates with 500 μl of RPMI 1640 containing 10% FCS and a 1% agarose underlay. After 7 days, cultures were resuspended in 0.2 ml of RPMI 1640 containing the same viruses at the same doses. Anchorage-independent growth was allowed to occur for 2 weeks, and colonies >125 μm in diameter were counted.

Inhibition of Tumor Growth *in Vivo*. The effect of Ad5CMV-BP3 on established s.c. tumor nodules was determined in athymic nude mice in a defined pathogen-free environment. Briefly, mice were irradiated with 350 rad (^{137}Cs source), and H1299 cells in 100 μl of complete medium were s.c. injected into the mice at a single dorsal site. After the tumor volume reached $\sim$75 mm^3, 1×10^{10} viral particles of Ad5CMV-BP3 or Ad5CMV in 100 μl of 1× PBS, or 100 μl of 1× PBS alone as a control, was intratumorally injected. Tumor size and volume were measured every day for 17 days after injection. Mice showing necrotic tumors or tumors $\geq$1.5 cm in diameter were euthanized. Results were expressed as the mean ($\pm$SD) tumor volume (calculated from five mice) relative to the tumor volume at the time of adenovirus injection (day 0).

Apoptosis Analysis. Apoptosis was measured using the APO-BRDU staining kit (Phoenix Flow Systems, San Diego, CA) as previously described (23). Briefly, H1299 cells were untreated or infected with Ad5CMV or Ad5CMV-BP3 and then allowed to grow in serum-free medium or medium containing 10% serum or 100 ng/ml IGF-I for 3 days. Floating and adherent cells were analyzed using a FACScan flow cytometer (Becton Dickinson, San Jose, CA) to determine the percentage of apoptotic cells. The percentage of dead cells was determined by FACS analysis of propidium iodide-stained nuclei. Apoptosis was also determined by detecting of nucleosomal DNA fragmentation, which was measured using the TACS apoptotic DNA laddering kit (Trevigen, Inc., Gaithersburg, MD) according to the manufacturer's protocol. Briefly, DNA was isolated from untreated or virus-infected H1299 cells by incubating the cells in lysis buffer. DNA samples were then subjected to electrophoresis on a 1.5% agarose gel and visualized by ethidium bromide staining. To determine whether Ad5CMV-BP3-induced apoptosis was mediated through the inhibition of the PI3K/Akt/PKB and MAPK pathways, 2×10^5 H1299 cells were seeded onto six-well plates and transiently transfected with 2 μg of an expression construct containing constitutively active Akt (MyrAkt) or constitutively active MAPKK (MEK1/R4F) using the FuGENE 6 transfection reagent (Roche Molecular Biochemicals) according to the manufacturer's protocol. After 4 h of transfection, H1299 cells were infected for 2 h with 1×10^4 particles/cell of Ad5CMV-BP3 or Ad5CMV as a control. Cells were changed to fresh RPMI 1640 containing 10% FCS and grown for 3 days. Apoptosis was measured using the APO-BRDU staining kit as described above.

Immunofluorescence Confocal Microscopy. To determine whether Ad5CMV-BP3 induced IGFBP-3 expression and apoptosis in tumor nodules in nude mice, 1×10^{10} viral particles of Ad5CMV-BP3 or Ad5CMV were intratumorally injected as described above, and tumor tissues were collected from the mice 3 days later. Tissues were fixed with 10% formaldehyde and embedded in paraffin. Then, 5-μm-thick tumor tissue sections were analyzed for IGFBP-3 expression and apoptosis-induced DNA fragmentation. Briefly, sections were deparaffinized through a series of xylene baths and rehydrated through graded ethanol baths. Next, the sections were treated with 2.5% blocking serum to reduce nonspecific binding and were incubated with primary antihuman IGFBP-3 rabbit polyclonal antibody, 1:100 dilution, and followed by incubation with Fluorolink Cy3-labeled secondary antibody. Paraffin-embedded tissue sections were analyzed for DNA fragmentation by TUNEL assay according to the manufacturer's protocol (Roche Molecular Biochemicals). Samples were analyzed using an inverted confocal microscope (Zeiss, Inc., Jena, Germany) operated by KS400 software (Zeiss, Inc.).

Immune Complex Kinase Assay. Immune complex kinase assays were performed as previously described (24). Briefly, untreated or virus-infected H1299 cells were grown for 2 days in RPMI 1640 containing 10% serum. After being washed with 1× PBS to eliminate residual serum, cells were serum starved for 1 day, activated by treatment with 50 ng/ml IGF-I for 15 min, and harvested using lysis buffer. Next, 100 μg of cell extracts were immunoprecipitated with a mixture of antibodies against p44 MAPK (ERK1)/p42 MAPK (ERK2) and with protein A-G agarose beads. After the beads were washed, an immune complex kinase assay was performed using MBP as a substrate.

RESULTS

IGFBP-3 Expression in NSCLC Cells Transduced by Ad5CMV-BP3. Induction of IGFBP-3 expression by Ad5CMV-BP3 was analyzed by Western blot analysis on H1299, H661, H441, H358, H226Br, H226B, and Calu6 NSCLC cell lines, which showed very low or no IGFBP-3 protein expression (data not shown). Representative results showing viral dose-dependent increase in IGFBP-3 protein level (M_r 42,000 and M_r 44,000 forms) in H1299 cells (C) or secreted into medium (S) are shown in Fig. 1*A*. IGFBP-3 expression was not detectable in the cells incubated with medium alone or with Ad5CMV. The expression of IGFBP-3 peaked at day 3 and decreased at day 5. These results are consistent with those of previous reports that showed maximal adenovirus-mediated gene expression at day 3 and rapid decrease after day 5 (25). The expression pattern in other NSCLC cell lines infected with Ad5CMV-BP3 was consistent with that in H1299 cells (data not shown). The Western ligand blot analysis using conditioned media from H1299 cells infected with Ad5CMV-BP3 or with Ad5CMV indicated that IGFBP-3 secreted from Ad5CMV-BP3-infected H1299 cells bound strongly to IGF-I (Fig. 1*B*) and IGF-II (data not shown).

Effect of IGFBP-3 on NSCLC Cell Growth. The effect of IGFBP-3 on IGF-induced NSCLC cell growth was investigated by MTT assay. IGF-I concentrations >10 ng/ml induced the growth of NSCLC cell lines (Fig. 2*A*), showing the mitogenic effect of IGF-I on NSCLC cells. IGF-II showed a minimal mitogenic effect on NSCLC cell growth (data not shown). Hence, we investigated the effects of Ad5CMV-BP3 on IGF-I-stimulated NSCLC cell growth. Relative to the control, Ad5CMV-BP3 infection inhibited IGF-I-induced growth of NSCLC cells in a viral dose-dependent manner. In contrast, Ad5CMV-BP3 showed minimal inhibitory effects on NSCLC cell growth in the absence of IGF-I. Importantly, Ad5CMV-BP3 was not detectably cytotoxic to NHBE cells regardless of the stimulation of IGF-I (Fig. 2*B*). Previous studies have suggested that IGF-1R is particularly important in anchorage-independent growth and that its inhibition also suppresses tumorigenicity (26, 27). Therefore, anchorage-independent growth of H1299 cells infected with Ad5CMV-BP3 was assessed by counting colony formation in soft agar. Relative to the effect of controls, Ad5CMV-BP3 infection prominently inhibited

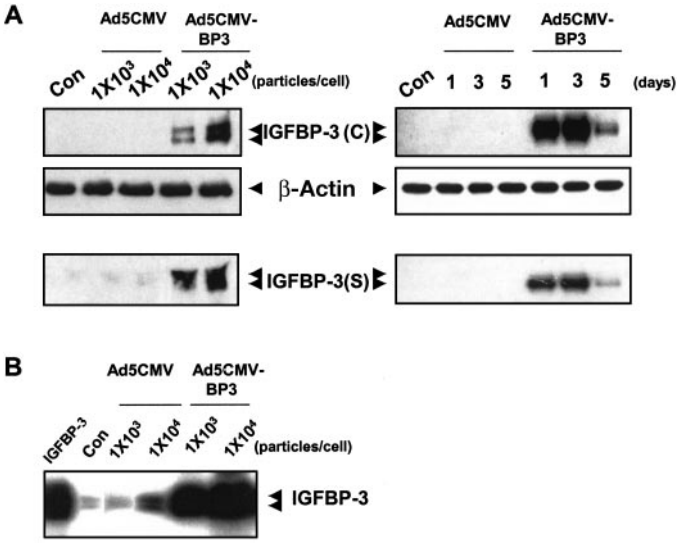

Fig. 1. Ad5CMV-BP3 infection increases IGFBP-3 expression in NSCLC cell lines. *A*, whole-cell lysates isolated from the indicated NSCLC cell lines were subjected to Western blot analysis for IGFBP-3 expression. *B*, H1299 NSCLC cells were untreated (*Con*) or infected with the indicated titers (particles/cell) of Ad5CMV-BP3 or the parental vector Ad5CMV for 3 days. IGFBP-3 in the cell (*C*) or secreted into the medium (*S*) was detected by Western blot analysis. The time course of IGFBP-3 expression was determined in H1299 cells that were untreated (*Con*) or infected with 1×10^4 particles/cell of Ad5CMV-BP3 or Ad5CMV. β-Actin was used as a loading control. *C*, Western ligand blot analysis was performed on conditioned media from cells infected with the indicated dose of Ad5CMV-BP3 or Ad5CMV for 3 days, using ^{125}I-labeled IGF-I as a probe. Recombinant IGFBP-3 (20 ng) was used as a positive control. The positions of specific forms of IGFBP-3 are indicated.

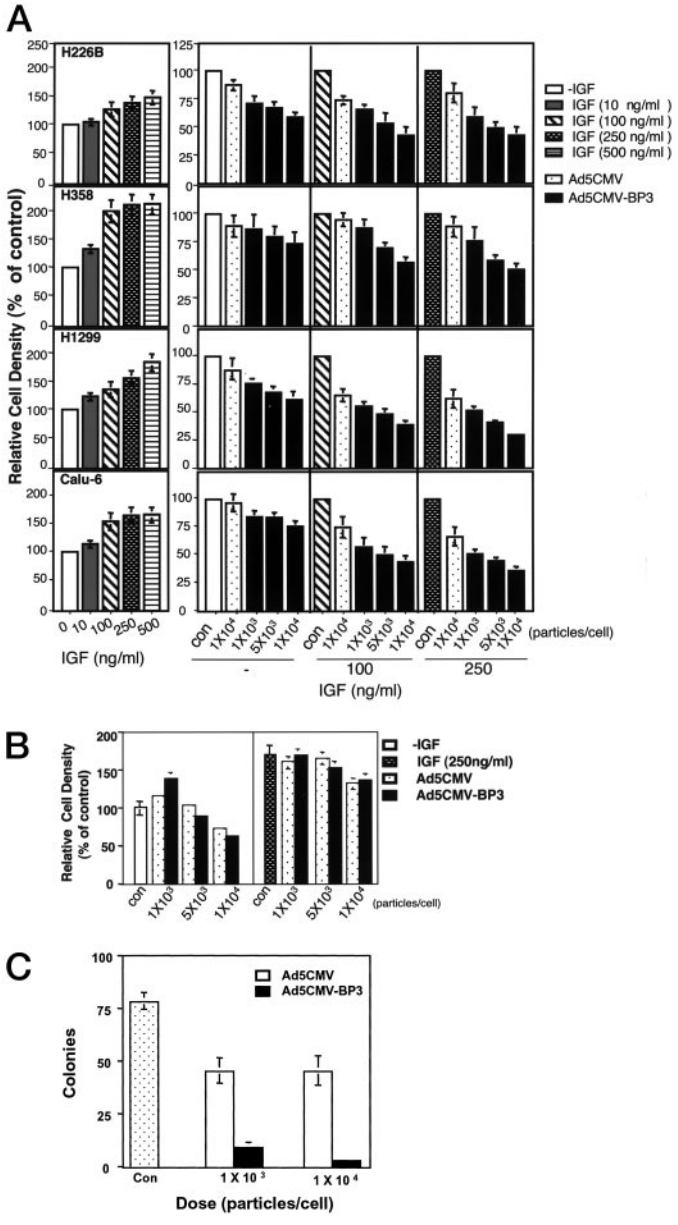

Fig. 2. Ad5CMV-BP3 inhibits the growth of NSCLC cells. *A*, *left*, the effects of IGF-I on the growth of indicated NSCLC cell lines were measured by MTT assays of cells incubated in serum-free medium with or without indicated doses of IGF-I for 3 days. Results are expressed relative to the density of cells incubated in serum-free medium. *Right*, the same cell lines were infected with the indicated doses (particles/cell) of Ad5CMV-BP3 or Ad5CMV and incubated in a serum-free medium with or without 100 or 250 ng/ml IGF-I. Results are expressed relative to the density of untreated cells incubated in a same medium that is either serum-free or containing 100 or 250 ng/ml IGF-I, respectively. *B*, the effects of IGF-I on the growth of NHBE cells were measured by MTT assays of cells infected with the indicated doses (particles/cell) of Ad5CMV-BP3 or Ad5CMV and incubated in a serum-free medium with or without 250 ng/ml IGF-I. MTT assays on infected cells were performed after 3 days of incubation. Results are expressed relative to the density of cells incubated in serum-free medium. Each value is the mean from six identical wells; *bars*, SD. *C*, the effect of Ad5CMV-BP3 on anchorage-independent growth of H1299 cells were investigated by plating the infected cells in RPMI 1640 containing 0.2% agarose on top of a base of 0.5% agarose in the culture medium. After 1 week, cells were infected again with the same dose of adenovirus. After 2 weeks, colonies >125 μm in diameter were counted under a microscope. Each value represents the mean from three independent experiments; *bars*, SD.

colony formation of H1299 cells in soft agar, with a 90% decrease in cells infected with 1×10^4 particles/cell of Ad5CMV-BP3 (Fig. 2*C*). These findings suggested that Ad5CMV-BP3 is capable of suppressing the tumorigenicity of H1299 NSCLC cells.

Inhibition of Tumor Growth *in Vivo*. To further investigate the growth-regulatory effects of IGFBP-3 in an *in vivo* setting, we determined the effect of Ad5CMV-BP3 on established s.c. tumor nodules in athymic nude mice. Once H1299 xenograft tumors reached a volume of at least 75 mm^3, 1×10^{10} viral particles of Ad5CMV-BP3 or Ad5CMV in 1× PBS or 1× PBS alone as a control was intratumorally injected, and tumor size was measured every day for 17 days. Ad5CMV-BP3 injection significantly reduced tumor volume (mean volume, 678.5 ± 195.5 mm^3), when compared with tumors injected with Ad5CMV (mean volume, 1291.5 ± 49.7 mm^3) or 1 × PBS (mean volume, 1305 ± 157 mm^3). The mean size of Ad5CMV-BP3-injected tumors was reduced by 48% by day 17 (Fig. 3).

Induction of Apoptosis by IGFBP-3 *in Vitro* and *in Vivo*. We investigated the mechanism by which IGFBP-3 inhibited NSCLC cell growth. Because IGFBP-3 is a potent inducer of apoptosis (4–7), evidence for apoptosis after Ad5CMV-BP3 was examined. Indeed, NSCLC cells infected with Ad5CMV-BP3 shrank and detached from their culture dishes (data not shown). Flow cytometric analysis of H1299 cells revealed that Ad5CMV-BP3 infection induced a comparable increase in incorporation of Br-dUTP, with 30.2% of the cells infected, and 1×10^4 particles/cell of Ad5CMV-BP3 were apoptotic (Fig. 4*A*). DNA fragmentation analysis on H1299 cells infected with 1×10^4 particles/cell of Ad5CMV-BP3 showed DNA ladders (Fig. 4*B*). Because the Bcl protein family has an important role in apoptosis, we examined the level of Bcl-2 and Bax in Ad5CMV-BP3-infected H1299 cells using Western blot analysis. Ad5CMV-BP3 inhibited the expression of Bcl-2 in a dose-dependent manner without changing the level of Bax, suggesting a role of IGFBP-3 in modulating the Bax:Bcl-2 ratio (Fig. 4*C*). Western blot analysis was also performed to determine whether Ad5CMV-BP3 induced a loss of the caspase-3 proenzyme (M_r 32,000) and cleavage of PARP, a substrate of caspase-3 proteolysis. H1299 cells infected with 1×10^4 particles/cell of Ad5CMV-BP3 for 3 days showed a significant decrease in the

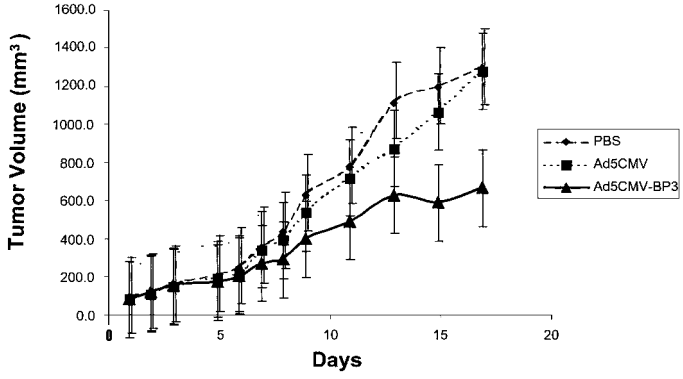

Treatment	Mean Volume (mm^3 ± SD)
PBS	1305.7 ± 157
Ad5CMV	1291.5 ± 49.7
Ad5CMV-BP3	678.5 ± 195.5

Fig. 3. Growth of NSCLC xenografts is inhibited by injection of Ad5CMV-BP3. H1299 cells were injected into the dorsal flank of athymic nude mice. Once tumor volume reached ~75 mm^3, 1×10^{10} viral particles of the indicated adenovirus or buffer alone (PBS) as a control was intratumorally injected. Tumors were measured every day, and results were expressed as the mean tumor volume (calculated from five mice) relative to the tumor volume at the time of adenoviral injection (day 0); *bars*, SD.

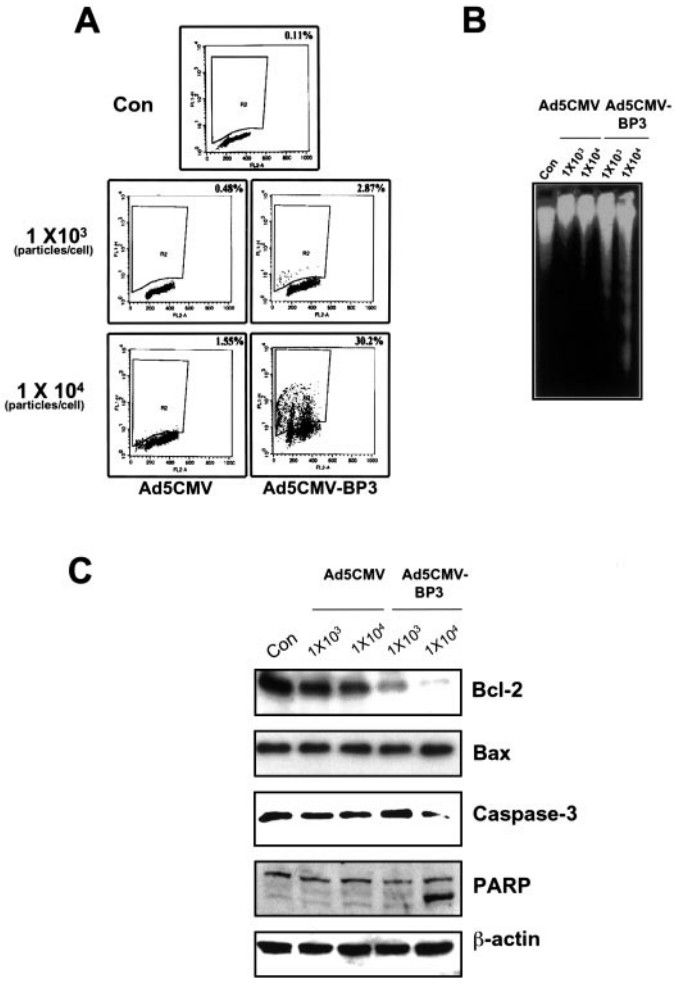

Fig. 4. IGFBP-3 induces apoptosis in NSCLC cells. *A*, flow cytometry was performed in H1299 cells infected with Ad5CMV-BP3 or Ad5CMV using APO-BRDU staining. Living gating of the forward and orthogonal scatter channels was used to exclude debris and to selectively acquire cell events. All values reflect the percentage of cells as determined by light scatter. The percentage of dead cells was determined by FACS analysis of propidium iodide-stained nuclei. *B*, nucleosomal DNA fragmentation analysis was performed on DNA isolated from untreated (*Con*), Ad5CMV-infected, and Ad5CMV-BP3-infected H1299 cells. *C*, the regulation of Bcl-2, Bax, and caspase-3 proenzyme (M_r 32,000) and the cleavage of PARP by Ad5CMV-BP3 were examined by Western blot analysis on H1299 cells infected with the indicated doses of adenovirus for 3 days.

M_r 32,000 caspase-3 proenzyme and in induction of the M_r 89,000 fragment of PARP cleaved from the M_r 113,000 form of PARP. These findings indicate that IGFBP-3 is a potent inducer of apoptosis in NSCLC cell lines. To further investigate whether induction of IGFBP-3 caused apoptosis *in vivo*, immunofluorescence analysis and TUNEL assay were performed on tumors that were removed 3 days after a single administration of adenovirus. Compared with the effect of Ad5CMV, Ad5CMV-BP3 injection markedly increased IGFBP-3 and TUNEL staining (Fig. 5), indicating that the expression of IGFBP-3 induced apoptosis in tumor tissues. Only minimal TUNEL staining occurred in the Ad5CMV-injected tumors, probably because of the toxicity of the empty virus. Confocal microscopy revealed that IGFBP-3 expression and DNA fragmentation were colocalized, indicating that the expression of IGFBP-3-induced apoptosis. Some regions showed strong TUNEL staining but no staining for IGFBP-3; this apoptosis may have been spontaneous or induced by IGFBP-3 that was degraded after induction of apoptosis.

Modulation of the PI3K and MAPK Pathways by IGFBP-3 in NSCLC Cells. IGFBP-3 has the potential to function as an antagonist of the PI3K and MAPK pathways because these pathways are acti-

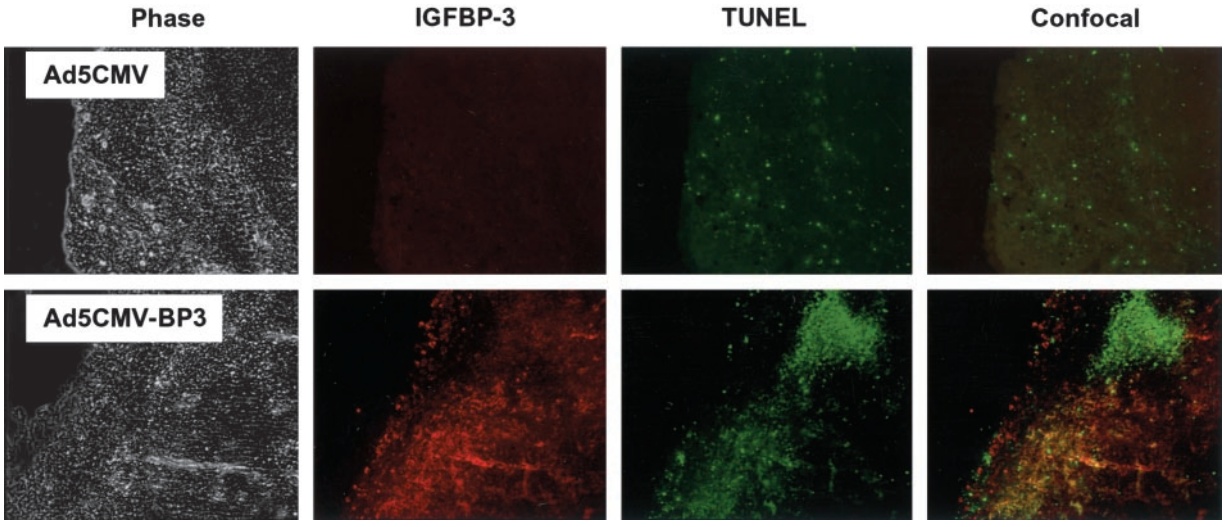

Fig. 5. IGFBP-3 expression and apoptosis are induced in NSCLC tumor xenografts after a single injection of Ad5CMV-BP3. Immunocytochemical analyses for IGFBP-3 expression and TUNEL analysis were performed on the tissues from H1299 cell-induced tumor nodules injected with Ad5CMV-BP3 or Ad5CMV. The cells positive upon staining for IGFBP-3 and for apoptosis are identified by *red* and *green* fluorescence, respectively.

vated by the IGF-I-induced signaling transduction mechanism (5). To address this possibility, we determined the effect of Ad5CMV-BP3 on the PI3K and MAPK pathways in Ad5CMV-BP3-infected H1299 cells. Activation of the PI3K pathway generally causes selective phosphorylation of a downstream effector, such as Akt at Ser-473/Thr-308 and GSK-3α/β at Ser-9/21 (28); therefore, we examined the levels of pAkt (Ser-473) and pGSK-3β (Ser-9) as surrogates for PI3K activity. According to results of Western blot analysis and an immune complex kinase assay, treatment with 50 ng/ml IGF-I for 15 min increased the levels of pAkt and pGSK-3β and induced MAPK activity in H1299 cells (Fig. 6, *A* and *B, left*). Ad5CMV-BP3 inhibited IGF-I-induced phosphorylation of Akt (Ser-473) and GSK-3β (Ser-9) in H1299 cells in a dose-dependent manner, whereas the levels of pAkt (Ser-473) and pGSK-3β (Ser-9) were not affected by IGF-I in untreated and Ad5CMV-infected H1299 cells (Fig. 6*A*). The total protein levels of Akt and GSK-3β were not changed by these treatments.

According to the immune complex kinase assay, Ad5CMV-BP3 infection also decreased MAPK activity without changing the protein levels of p44 MAPK (ERK1) and p42 MAPK (ERK2) in H1299 cells (Fig. 6*B*), suggesting that IGFBP-3 suppressed the IGF-I-induced activation of the PI3K/Akt/PKB and MAPK pathways in H1299 cells.

Overexpression of Constitutively Active Akt or MEK1 Protects H1299 Cells from IGFBP-3-induced Apoptosis. We investigated whether IGFBP-3 inhibits IGF-induced cell survival pathways in NSCLC cells. Evidence of apoptosis was assessed in H1299 cells, which were untreated or infected with Ad5CMV or Ad5CMV-BP3 and then allowed to grow in the absence or presence of IGF-I. According to flow cytometric analysis, IGF-I treatment rescued H1299 cells from serum depletion-induced apoptosis in H1299 NSCLC cells. However, this rescue was blocked by the overexpression of IGFBP-3 (Fig. 7*A*), suggesting that IGFBP-3 interferes with survival function of IGF-I. To further explore whether IGFBP-3-induced apoptosis was mediated through the inhibition of IGF-I-induced signaling pathways, the susceptibility to the induction of apoptosis by Ad5CMV-BP3 was assessed in H1299 cells transfected with constitutively active Akt (MyrAkt) or constitutively active MEK1 (R4F) followed by the infection with Ad5CMV-BP3 or Ad5CMV. The equal transfection in each condition was verified by Western blot analysis on MyrAkt and MEK1 (data not shown). According to flow cytometry analysis, 10.4% of MyrAkt-transfected H1299 cells and 27.9% of MEK1-transfected cells showed induction of apoptosis by 1×10^4 particles/cell of Ad5CMV-BP3, as compared with 43% of induction in pCMV (empty vector)-transfected cells (Fig. 7*B*), suggesting that the induction of apoptosis by IGFBP-3 in NSCLC cells was attributable in part to the inhibition of the IGF-induced PI3K/Akt/PKB and MAPK pathways. Taken together, these results suggested a crucial role of IGFBP-3 in PI3K/Akt/PKB and MAPK-mediated cell survival pathways.

DISCUSSION

Previous studies have shown that IGFs are potent mitogens in several NSCLC and SCLC cells (29–31). Therapeutic strategies designed to interfere with IGF-I-mediated signal transduction, such as soluble IGF-1R, anti-IGF-IR antibody, and an adenovirus vector expressing IGF-1R, show antitumor effects of IGF-1R inhibition (26, 27). In addition, IGFBPs play a role in regulating cell growth by competitively binding IGFs and preventing their binding to IGF-1R (2, 3, 17–19). We have demonstrated previously that adenovirus

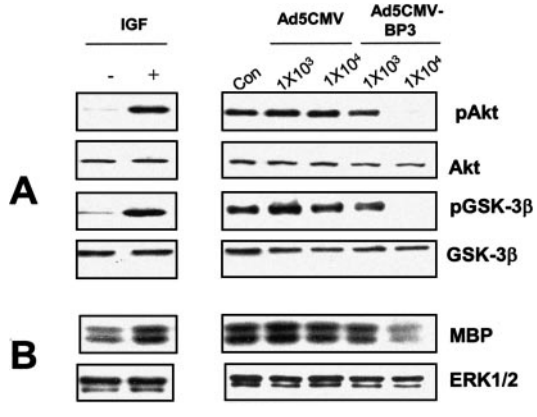

Fig. 6. IGFBP-3 inhibits the PI3K and MAPK pathways in NSCLC cells. The levels of pAkt, pGSK-3β (*A, left*), and the activity of MAPK (*B, left*) in H1299 cells untreated (−) and stimulated by IGF-I (+) were examined by Western analysis and immune complex kinase assay using MBP, respectively. *A*, the expression of pAkt (Ser-473), Akt, pGSK-3β (Ser-9), and GSK-3β were measured by Western blot analysis in H1299 cells untreated (*Con*) or infected with the indicated dose of adenovirus. *B*, MAPK activity was determined by an immune complex kinase assay using MBP. Total ERK1/2 expression was examined by Western blot analysis.

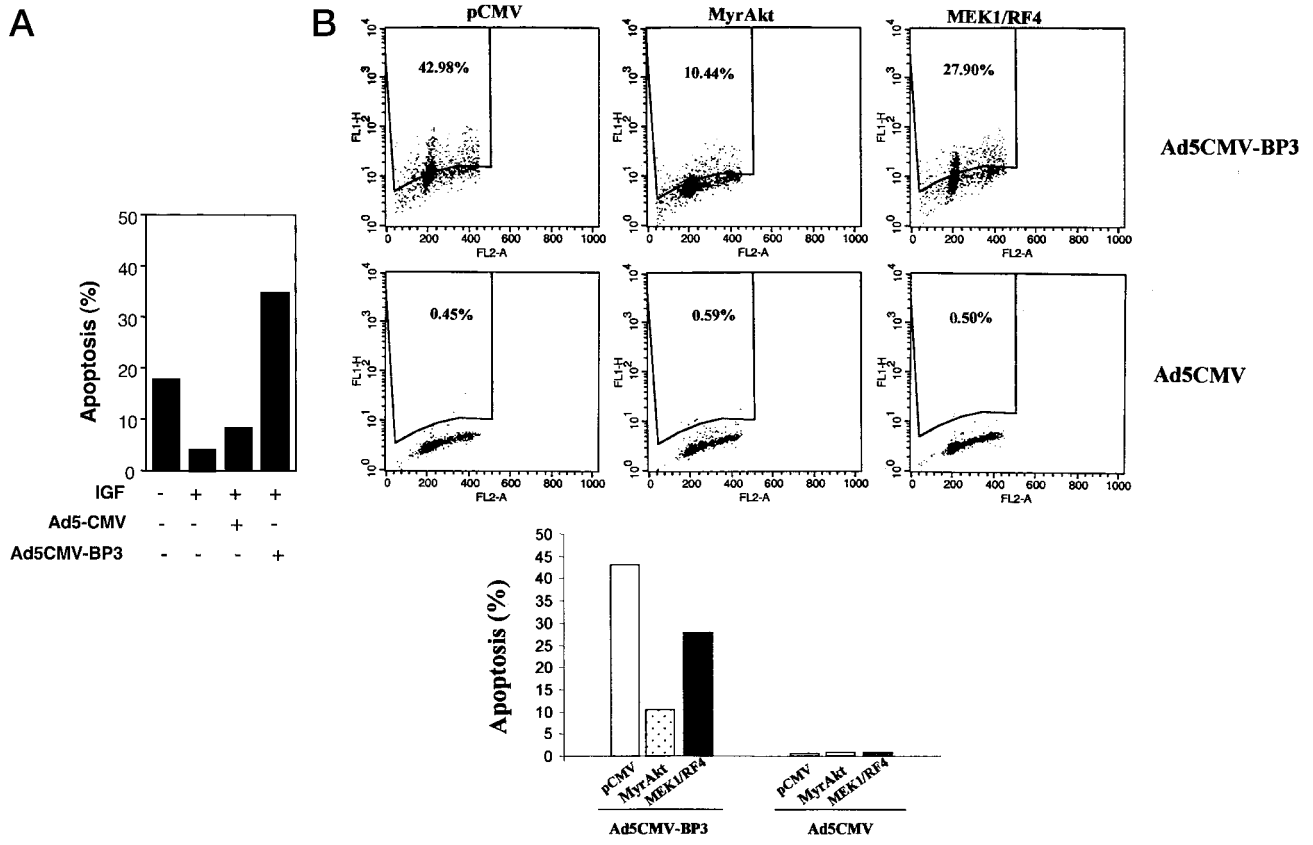

Fig. 7. *A*, IGFBP-3 interferes with the survival function of IGF-I. Apoptosis was measured in H1299 cells, which were untreated or infected with Ad5CMV or Ad5CMV-BP3 and then allowed to grow in serum-free medium containing 100 ng/ml IGF-I for 3 days. Floating and adherent cells were analyzed using a FACScan flow cytometer (Becton Dickinson, San Jose, CA) to determine the percentage of apoptotic cells. Results are expressed relative to the apoptosis of cells incubated in serum-free medium for 3 days. At least three independent experiments were performed with similar results. *B*, activated Akt/PKB or MAPKK (MEK)-1 protects H1299 cells from IGFBP-3-induced apoptosis. Induction of apoptosis by 1×10^4 particles/cell of Ad5CMV-BP3 in H1299 cells transfected with the control pCMV vector or constitutively active Akt (*MyrAkt*) or constitutively active MAPKK (*MEK1/R4F*) was analyzed by flow cytometry using APO-BRDU staining. No appreciable change was noted in Ad5CMV-infected H1299 cells transfected with any of these expression vectors. *Columns*, the amounts of apoptosis in H1299 cells transfected with respective expression constructs after the infection of 1×10^4 particles/cell of Ad5CMV-BP3 or Ad5CMV.

expressing IGFBP-6 (Ad5CMV-BP6) reduces the growth of NSCLC cells *in vitro* and *in vivo* (23). However, because IGFBP-6 binds with higher affinity to IGF-II than to IGF-I and because IGFBP-3 is the most abundant IGFBP in human serum, we investigated the effects of IGFBP-3 on the growth of NSCLC cells using a recombinant adenovirus that expresses IGFBP-3 under the control of a CMV promoter (Ad5CMV-BP3).

After we confirmed the function of Ad5CMV-BP3 in induction of IGFBP3 expression by Western blot and in binding of secreted IGFBP-3 to IGF-I and IGF-II by Western ligand blot analysis, we investigated the growth inhibitory effects of IGFBP-3. IGFs stimulated the growth of a subset of NSCLC cell lines, a result in agreement with previous findings (30) that showed a 1.1–2.7-fold increase in cell number stimulated by IGF-1 in a panel of NSCLC lines. The effects of IGF-I on NSCLC cell growth were relatively modest, with the exception of H358 cells, compared with the values reported for other models. This may be related to the fact that lung tumor cells with functional IGF receptors are able to enhance their own growth by synthesis of endogenous IGFs (31). Thus, exogenous IGFs may induce only a modest increase of NSCLC cell growth. Ad5CMV-BP3 inhibited the IGF-I-stimulated growth of these cells, which is consistent with previous findings that showed an IGF-dependent, growth-inhibitory effect of IGFBP-3 in human breast cancer cells (27). However, Hochscheid *et al.* (32) found that IGFBP-3 induced IGF-independent growth inhibition in a NSCLC cell line, observing that a higher concentration of IGF-I did not influence the proliferation of NSCLC cells stably transfected with IGFBP-3. The difference in these results might have been attributable to cell type specificity or different model systems used in the studies. In addition, stable transfection of IGFBP-3 might cause IGF-independent cell growth, and the growth of stably transfected cells could be regulated directly by IGFBP-3.

The crucial roles of IGF-1R in the establishment and maintenance of the transformed phenotype have been underscored (23, 28, 29). In our study, infection of Ad5CMV-BP3 decreased the clonogenicity of H1299 cells in soft agar by >90%, which was comparable with the 84% decrease by an adenovirus expressing antisense IGF-1R (23). Furthermore, the growth of NSCLC tumors established in nude mice was decreased by the injection of Ad5CMV-BP3, indicating that IGFBP-3 overexpression inhibits the growth of NSCLC cells *in vitro* and *in vivo*. These dramatic effects of IGFBP-3 could be caused by combined IGF-dependent suppression of IGF-1R signaling and direct IGF-independent effects, possibly mediated via retinoid X receptor (9).

IGFs are known to protect cells from a variety of apoptotic stimuli through an IGF-1R-mediated cell survival pathway. Studies have shown that overexpression of IGF-1R protects cells against apoptosis, that suppression of IGF-1R induces apoptosis (5), and that the sequestration of IGFBP-3 of IGFs away from IGF-1R induces apoptosis (5–7, 16). On the basis of these results, we hypothesized that IGFBP-3 acts as an effector of apoptosis in NSCLC cells by inhibiting IGF-I-mediated cell survival, antiapoptotic pathways, or both. In fact, we found evidence showing that Ad5CMV-BP3 induced apoptosis in NSCLC cells *in vitro* and *in vivo*, and that activity of Akt/PKB and MAPK, mediators of IGF-induced signaling pathways, were sup-

pressed by overexpression of IGFBP-3. It has been demonstrated that Akt/PKB and MAPK have potent inhibitory effects on apoptosis (33). Activation of IGF-1R by IGFs has been associated with an abrogation of caspase-3, caspase-7, and caspase-1 activity and changes in both proapoptotic and antiapoptotic members of the Bcl-2 family in a variety of cell systems (33, 34). The serine-threonine protein kinase Akt, a downstream mediator of the PI3K pathway, is also involved in phosphorylation of the proapoptotic protein BAD, releasing BAD from heterodimerization with cytoprotective proteins, such as Bcl-2 and Bcl-x_L, thereby inhibiting its proapoptotic activity (4, 33, 34). It is plausible that the IGF-dependent effects of IGFBP-3 reverse these actions and that IGFBP-3 therefore acts as an effector of apoptosis. We found that apoptosis induced by serum depletion of H1299 NSCLC cells were rescued by IGF-I treatment. However, this rescue was blocked by overexpression of IGFBP-3. Furthermore, constitutively active Akt or constitutively active MAPKK partially blocked the apoptosis induced by Ad5CMV-BP3, suggesting that IGFBP-3 induces apoptosis in NSCLC cells, in part via inhibition of the IGF-I-induced PI3K/Akt/PKB and MAPK pathways. This report is the first to show that IGFBP-3 induces apoptosis in NSCLC cells via inhibition of the signal transduction mechanism involved in cellular proliferation and survival.

The role of IGFBP-3 as an inhibitor of Akt/PKB activation has particular clinical implications, especially in the treatment of NSCLC, where constitutive activation of Akt/PKB occurs at a high frequency (35). The role of Akt/PKB in survival has been demonstrated in studies in which cells were exposed to different apoptotic stimuli such as UV irradiation, growth factor withdrawal, cell cycle discordance, DNA damage, and TGF-β (36–39). Manipulating Akt/PKB activity alters the sensitivity of cells to chemotherapy and irradiation; addition of a PI3K inhibitor or transfection of kinase-dead Akt/PKB into cells with high levels of Akt/PKB activity causes dramatic sensitization to these treatments (35). Therefore, targeting Akt/PKB by using Ad5CMV-BP3 can enhance the efficacy of chemotherapy and radiation therapy and increase the apoptotic potential of NSCLC cells.

In conclusion, our study produced several important findings:

(*a*) We demonstrated that delivery of IGFBP-3 via a recombinant adenovirus inhibits lung cancer cell growth *in vitro* and reduces tumor growth *in vivo* via induction of apoptosis.

(*b*) We demonstrated that Ad5CMV-BP3 has no cytotoxicity on NHBE cells, suggesting a therapeutic potential of IGFBP-3. However, the nonspecific toxicity demonstrated by reduction in cell number and agar colonies at high titers of control virus (Ad5CMV) may be an obstacle to use Ad5CMV-BP-3 in clinical trials, despite the significant activity of Ad5CMV-BP3 in the regulation of cell growth.

(*c*) We demonstrated that adenoviral IGFBP-3 inhibits the MAPK and PI3K pathways, which have important roles in cell proliferation and survival. These results suggest that IGFBP-3 is an attractive target for lung cancer therapy and that Ad5CMV-BP3, as well as other therapeutic tools including small molecules targeting IGF-I:IGFBP-3 interaction, should be considered for clinical application. Important questions that remain are how to overcome the transient effect of adenoviral vector-induced gene expression, how to target more specifically to the site of tumors, and how to minimize the cytotoxicity of the adenoviral vector and the neutralizing effect of the antibodies that may arise in animals or patients after viral treatment.

REFERENCES

1. Mitsudomi, T., Steinberg, S. M., Nau, M. M., Carbone, D., D'Amico, D., Bodner, S., Oie, H. K., Linnolila, R. I., Mulshine, J. L., Minna, J. D., and Gazdar, A. F. *p53* gene mutations in non-small-cell lung cancer cell lines and their correlation with the presence of ras mutations and clinical features. Oncogene, *7:* 171–180, 1992.
2. Nemunaitis, J., Swisher, S. G., Timmons, T., Connors, D., Mack, M., Doerksen, L., Weill, D., Wait, J., Lawrence, D. D., Kemp, B. L., Fossella, F., Glisson, B. S., Hong, W. K., Khuri, F. R., Kurie, J. M., Lee, J. J., Lee, J. S., Nguyen, D. M., Nesbitt, J. C., Perez-Soler, R., Pisters, K. M. W., Putnam, J. B., Richli, W. R., Shin, D. M., Walsh, G. L., Merritt, J., and Roth, J. Adenovirus-mediated *p53* gene transfer in sequence with cisplatin to tumors of patients with non-small cell lung cancer. J. Clin. Oncol., *18:* 609–622, 2000.
3. Brodt, P., Samani, A., and Navab, R. Inhibition of the type-I insulin-like growth factor receptor expression and signaling: novel strategies for antimetastatic therapy. Biochem. Pharmacol., *60:* 1101–1107, 2000.
4. Lin, J., Adam, R. M., Santiestevan, E., and Freeman, M. R. The phosphatidylinositol 3′-kinase pathway is a dominant growth factor-activated cell survival pathway in LNCaP human prostate carcinoma cells. Cancer Res., *59:* 2891–2897, 1999.
5. Butt, A. J., Firth, S. M., King, M. A., and Baxter, R. Insulin-like growth factor binding protein-3 modulates expression of Bax and Bcl-2 and potentiates p53-independent radiation-induced apoptosis in human breast cancer cells. J. Biol. Chem., *275:* 39174–39181, 2000.
6. Yu, H., Spitz, M. R., Mistry, J., Gu, J., Hong, W. K., and Wu, X. Plasma levels of insulin-like growth factor-I and lung cancer risk: a case-control analysis. J. Natl. Cancer Inst., *91:* 151–156, 1999.
7. Rajah, R., Valentinis, B., and Cohen, P. Insulin-like growth factor (IGF)-binding protein-3 induces apoptosis and mediates the effects of transforming growth factor-β1 on programmed cell death through a p53- and IGF-independent mechanism. J. Cell Biol., *272:* 12181–12188, 1997.
8. Leal, S. M., Liu, Q., Huang, S. S., and Huang, J. S. The type V transforming growth factor β receptor is the putative insulin-like growth factor binding protein 3 receptor. J. Biol. Chem., *272:* 20572–20576, 1997.
9. Liu, B., Lee, H-Y., Weinzimer, S. A., Powell, D. R., Clifford, J. L., Kurie, J. M., and Cohen, P. Direct functional interactions between insulin-like growth factor (IGF)-binding protein-3 and retinoid X receptor-α regulate transcriptional signaling and apoptosis. J. Biol. Chem., *275:* 33607–33613, 2000.
10. Schedlich, L. J., Le Page, S., Firth, S. M., Briggs, L. J., Jans, D. A., and Baxter, R. C. Nuclear import of insulin-like growth factor binding protein-3 (IGFBP-3) and IGFBP-5 is mediated by the importin β subunit. J. Biol. Chem., *275:* 23462–23470, 2000.
11. Oh, Y., Mullers, H. L., Ng, L., and Rosenfeld, R. G. Transforming growth factor-β-induced cell growth inhibition in human breast cancer cells is mediated through insulin-like growth factor-binding protein-3. J. Biol. Chem., *270:* 13589–13592, 1995.
12. Rozen, F., Ahang, J., and Pollak, M. Antiproliferative action of tumor necrosis factor-α on MCF-7 breast cancer cells is associated with increased insulin-like growth factor binding protein-3 accumulation. Int. J. Oncol., *13:* 865–869, 1998.
13. Han, G-R., Dohi, D. F., Lee, H-Y., Rajah, R., Walsh, G. L., Hong, W. K., Cohen, P., and Kurie, J. M. All-*trans* retinoic acid increases transforming growth factor-β2 and insulin-like growth factor binding protein-3 expression through a retinoic acid receptor-α-dependent signaling pathway. J. Biol. Chem., *272:* 13711–13716, 1997.
14. Huynh, H., Yang, X., and Pollak, M. Estradiol and antiestrogens regulate a growth-inhibitory insulin-like growth factor binding protein-3 autocrine loop in human breast cancer cells. J. Biol. Chem., *271:* 1016–1021, 1996.
15. Agarwal, C., Lambert, A., Chandraratna, R. A. S., Rorke, E. A., and Eckert, R. L. Vitamin D regulates human ectocervical epithelial cell proliferation and insulin-like growth factor binding protein-3 level. Biol. Reprod., *60:* 567–572, 1999.
16. Buckbinder, L., Talbott, R., Velasco-Miguel, S., Takenaka, I., Faha, B., Seizinger, B. R., and Kley, N. Induction of the growth inhibitor IGF-binding protein 3 by p53. Nature (Lond.), *377:* 646–648, 1995.
17. Cohick, W. S., and Clemmons, D. R. Enhanced expression of dihydrofolate reductase by bovine kidney epithelial cells results in altered cell morphology, IGF-I responsiveness, and IGF binding protein-3 expression. J. Cell. Physiol., *161:* 178–186, 1994.
18. Grill, C. J., and Cohick, W. S. Insulin-like growth factor-binding protein-3 mediates IGF-I action in bovine mammary epithelial cell line independent of an IGF interaction. J. Cell. Physiol., *183:* 273–283, 2000.
19. McCusker, R. H., Busby, W. H., Dehoff, M. H., Camacho-Hubner, C., and Clemmons, D. R. Insulin-like growth factor (IGF) binding to cell monolayers is directly modulated by the addition of IGF-binding proteins. Endocrinology, *129:* 939–949, 1991.
20. Campbell, P. G., Durham, S. K., Suwanichkul, A., Hayes, J. D., and Powell, D. R. Plasminogen binds the heparin-binding domain of insulin-like growth factor-binding protein-3. Am. J. Physiol., *275:* E321–E331, 1998.
21. Lee, H-Y., Dohi, D. F., Kim, Y-H., Walsh, G. L., Consoli, U., Andreef, M., Dawson, M. I., Hong, W. K., and Kurie, J. M. All-*trans* retinoic acid converts E2F into a transcriptional suppressor and inhibits the growth of human bronchial epithelial cells through a retinoic acid receptor-dependent signaling pathway. J. Clin. Investig., *101:* 1012–1019, 1998.
22. Sueoka, N., Lee, H-Y., Walsh, G. L., Fang, B., Ji, L., Roth, J. A., LaPushin, R., Hong, W. K., and Kurie, J. M. Insulin-like growth factor binding protein-6 inhibits the growth of human bronchial epithelial cells and increases in abundance with all-*trans* retinoic acid treatment. Am. J. Respir. Cell Mol. Biol., *23:* 297–303, 2000.
23. Sueoka, N., Lee, H-Y., Wiehle, S., Cristiano, R. J., Fang, B., Ji, L., Roth, J. A., Hong, W. K., Cihen, P., and Kurie, J. M. Insulin-like growth factor binding protein-6 activates programmed cell death in non-small cell lung cancer cells. Oncogene, *19:* 4432–4436, 2000.
24. Lee, H-Y., Walsh, G. L., Dawson, M. I., Hong, W. K., and Kurie, J. M. All-trans retinoic acid inhibits Jun-N-terminal kinase-dependent signaling pathway. J. Biol. Chem., *273:* 7066–7070, 1998.
25. Zhang, W-W., Fang, X., Mazur, W., French, B. A., Georges, R. N., and Roth, J. A. High efficiency gene transfer and high-level expression of wild-type p53 in human

lung cancer cells mediated by recombinant adenovirus. Cancer Gene Ther., *1:* 5–13, 1994.
26. Baserga, R. The IGF-I receptor in cancer research. Exp. Cell Res., *253:* 1–6, 1999.
27. Lee, C-T., Wu, S., Gabrilovich, D., Nada-Rahrov, S., Ciernik, I. F., and Carbone, D. P. Antitumor effects of an adenovirus expressing antisense insulin-like growth factor I receptor on human lung cancer cell lines. Cancer Res., *56:* 3038–3041, 1996.
28. Grimberg, A., and Cohen, P. Role of insulin-like growth factors and their binding proteins in growth and carcinogenesis. J. Cell. Physiol., *183:* 1–9, 2000.
29. Macaulay, V. M., Everard, M. J., Teale, J. D., Trott, P., Van Wyk, J. J., Smith, I. E., and Millar, J. L. Autocrine function for insulin-like growth factor-I and response to exogenous IGF-I in small cell lung cancer cell lines and fresh tumor cells. Cancer Res., *50:* 2511–2517, 1990.
30. Rotsch, M., Maasberg, M., Erbil, C., Jacques, G., Worsh, U., and Havemann, K. Characterization of insulin-like growth factor-I receptors and growth effects in human lung cancer cell lines. J. Cancer Res. Clin. Oncol., *118:* 502–508, 1992.
31. Minuto, F., Del Monte, P., Barreca, A., Alama, A., Cariola, G., and Giordano, G. Evidence for autocrine mitogenic stimulation by somatomedin-C/insulin-like growth factor-I on an established human lung cancer cell line. Cancer Res., *46:* 3716–3719, 1988.
32. Hochscheid, R., Jaques, G., and Wegmann, B. Transfection of human insulin-like growth factor-binding protein-3 gene inhibits cell growth and tumorigenicity: a cell culture model for lung cancer. J. Endocrinol., *166:* 553–563, 2000.
33. Krasilnikov, M. A. Phosphatidylinositol-3 kinase dependent pathways: the role in control of cell growth, survival, and malignant transformation. Biochemistry, *65:* 59–67, 2000.
34. Williams, A. C., Collard, T. J., Perks, C. M., Newcomb, P., Moorghen, M., Holly, J. M. P., and Paraskeva, C. Increased p53-dependent apoptosis by the insulin-like growth factor binding protein IGFBP-3 in human colonic adenoma derived cells. Cancer Res., *60:* 22–27, 2000.
35. Brognard, J., Clark, A. S., Ni, Y., and Dennis, P. A. Akt/Protein Kinase B is constitutively active in non-small cell lung cancer cells and promotes cellular survival and resistance to chemotherapy and radiation. Cancer Res., *61:* 3986–3997, 2001.
36. Kennedy, S. G., Kandel, E. S., Cross, T. K., and Hay, N. Akt/protein kinase B inhibits cell death by preventing the release of cytochrome *c* from mitochondria. Mol. Cell. Biol., *19:* 5800–5810, 1999.
37. Chen, R. H., Su, Y. H., Chuang, R. L., and Chang, T. Y. Suppression of transforming growth factor-β-induced apoptosis through a phosphatidylinositol 3-kinase/Akt-dependent pathway. Oncogene, *17:* 1959–1968, 1998.
38. Hausler, P., Papoff, G., Eramo, A., Reif, K., Cantrell, D. A., and Ruberti, G. Protection of CD95-mediated apoptosis by activation of phosphatidylinositide 3-kinase and protein kinase B. Eur. J. Immunol., *28:* 57–69, 1998.
39. Kulik, G., and Weber, M. J. Akt-dependent and -independent survival signaling pathways utilized by insulin-like growth factor I. Mol. Cell. Biol., *18:* 6711–6718, 1998.

Insulin-like Growth Factor Binding Protein-3 Inhibits the Growth of Non-Small Cell Lung Cancer

Ho-Young Lee, Kyung-Hee Chun, Bingrong Liu, et al.

Cancer Res 2002;62:3530-3537.